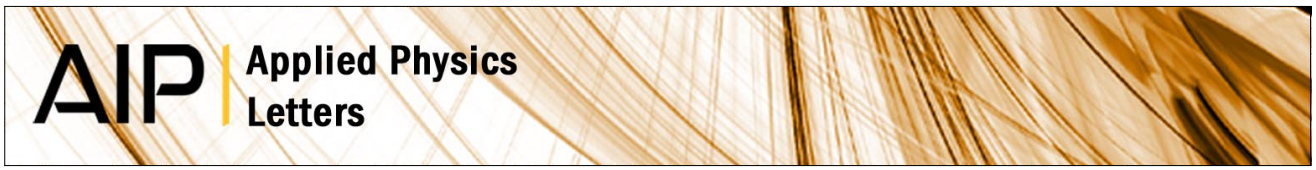

High-speed GaAs-based resonant-cavity-enhanced 1.3 μm photodetector

Ibrahim Kimukin, Ekmel Ozbay, Necmi Biyikli, Tolga Kartaloglu, Orhan Aytür et al.

Citation: Appl. Phys. Lett. **77**, 3890 (2000); doi: 10.1063/1.1329628
View online: http://dx.doi.org/10.1063/1.1329628
View Table of Contents: http://apl.aip.org/resource/1/APPLAB/v77/i24
Published by the American Institute of Physics.

High-speed GaAs-based resonant-cavity-enhanced 1.3 μm photodetector

Ibrahim Kimukin[a] and Ekmel Ozbay
Department of Physics, Bilkent University, Ankara 06533, Turkey

Necmi Biyikli, Tolga Kartaloğlu, and Orhan Aytür
Department of Electrical and Electronics Engineering, Bilkent University, Ankara 06533, Turkey

Selim Unlu
Department of Electrical and Computer Engineering, Boston University, Boston, Massachusetts 02215

Gary Tuttle
Microelectronics Research Center, Iowa State University, Ames, Iowa 50011

(Received 9 August 2000; accepted for publication 2 October 2000)

We report GaAs-based high-speed, resonant-cavity-enhanced, Schottky barrier internal photoemission photodiodes operating at 1.3 μm. The devices were fabricated by using a microwave-compatible fabrication process. Resonance of the cavity was tuned to 1.3 μm and a nine-fold enhancement was achieved in quantum efficiency. The photodiode had an experimental setup limited temporal response of 16 ps, corresponding to a 3 dB bandwidth of 20 GHz. © *2000 American Institute of Physics.* [S0003-6951(00)00149-2]

High-speed infrared photodetectors are becoming increasingly important for optical communication, signal processing, infrared imaging, and measurement systems. InGaAs and HgCdTe photodetectors are commercially available and most commonly used in communication and infrared imaging applications.[1] In addition to these detectors, quantum well infrared photodetectors (QWIP), and homojunction far-infrared photodiodes are also studied very extensively. QWIPs, resonant cavity enhanced SiGe/Si,[2,3] GaAs,[4,5] and Si homojunction[6,7] detectors became possible with the advent of the silicon and gallium arsenide molecular beam epitaxy growth techniques. PtSi and IrSi Schottky contact internal photoemission detectors for operation in the infrared and far infrared regions[8] are among the most promising sensors for large-scale monolithic infrared imaging arrays due to their compatibility with the standard Si or GaAs integrated circuit processing. In this letter, we report on GaAs based resonant cavity enhanced Schottky barrier internal photoemission photodetectors operating at 1.3 μm.

Resonant cavity enhanced (RCE) photodetectors offer the possibility of overcoming the low quantum efficiency limitation of conventional photodetectors.[9] The RCE detectors are based on the enhancement of the optical field within a Fabry–Perot resonator. The increased field allows the use of a thin absorbing layer, which minimizes the transit time of the photogenerated carriers without hampering the quantum efficiency. The enhancement of quantum efficiency with respect to a conventional detector is given by

$$\eta_{\text{enhancement}} = \frac{(1+R_2 e^{-\alpha d})}{1-2\sqrt{R_1 R_2}e^{-\alpha d}\cos(2\beta L+\phi_1+\phi_2)+R_1 R_2 e^{-2\alpha d}}, \tag{1}$$

where α is the absorption coefficient, d and L are the length of the active layer and the resonator, and R_1 and R_2 are the reflectivities of the top and the bottom mirrors.[9] The enhancement exceeds unity for the resonance frequencies of the cavity. High-speed RCE photodetector research has mainly concentrated on using p-i-n photodiodes and avalanche photodiodes, where 75% quantum efficiency was achieved along with a $>$20 GHz bandwidth.[10,11] Recently, we fabricated high-speed RCE p-i-n and Schottky photodetectors, where a 90% quantum efficiency along with a 3 dB bandwidth of 50 GHz has been reported.[12,13]

Internal photoemission is the optical excitation of electrons in the Schottky metal to an energy above the Schottky barrier and then transport of these electrons to the conduction band of the semiconductor (Fig. 1). In a gas of electrons obeying the Fermi–Dirac statistics the number of electrons per unit volume $n(u)du$ with velocity component normal to the surface in the range u, $u+du$ is given by

$$n(u)du = 2\left(\frac{m}{h}\right)^3 du \int_0^\infty \int_0^{2\pi} \frac{\rho d\rho d\theta}{e^{[1/2m(u^2+\rho^2)-E_F]/kT}+1}, \tag{2}$$

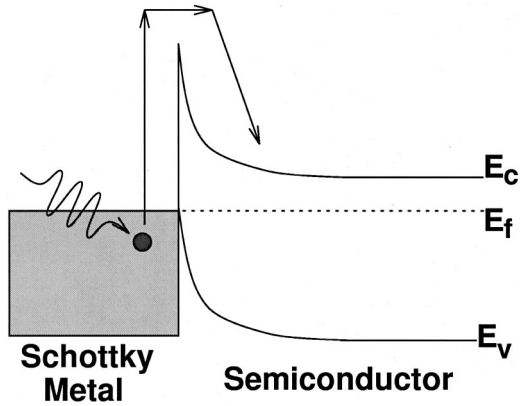

FIG. 1. Internal photoemission mechanism. Electrons in the Schottky metal are excited to an energy above the Schottky barrier and then they transport to the conduction band of the semiconductor.

[a]Electronic mail: kimukin@fen.bilkent.edu.tr

where E_F is the Fermi energy level, m is the electron mass, and T is the temperature. After evaluation of the integral, Eq. (2) can be expressed as

$$n(u)du = \frac{4\pi kT}{m}\left(\frac{m}{h}\right)^3 \log[e^{(E_F - 1/2mu^2)/kT} + 1]du. \quad (3)$$

According to the theory developed by Fowler, the number of electrons emitted per quantum of light absorbed is to a first approximation proportional to the number of electrons per unit volume of the metal whose kinetic energy normal to the surface is sufficient to overcome the potential step of the surface.[14,15] The number of electrons that can go over the Schottky barrier and contribute to the photocurrent is given by

$$N = \int_{1/2mu^2 = E_F + \phi_B - h\nu}^{\infty} n(u)du. \quad (4)$$

The internal quantum efficiency is proportional to the number of excited electrons to the conduction band. For the photon energies higher than the potential barrier, Eq. (4) can be approximated to obtain an expression for the internal quantum efficiency as a function of the photon energy

$$\eta \propto (h\nu - \phi_B)^2, \quad (5)$$

where ν is the photon frequency, and ϕ_B is the barrier height.

We used the transfer matrix method to design the epilayer structure and to simulate the optical properties of the photodiode. The epilayer structure of the photodiode was grown by a solid-source molecular beam epitaxy on a semi-insulating GaAs substrate. The bottom mirror was made from quarter-wave stacks of GaAs and AlAs designed for high reflectance at 1300 nm center wavelength. On top of the bottom mirror, a 300-nm-thick undoped GaAs layer was grown for mesa isolation. This layer was followed by a 600-nm-thick GaAs layer doped at $10^{18}\,\mathrm{cm}^{-3}$ for ohmic contact, and a lightly doped 200-nm-thick GaAs layer for the Schottky contact. Cavity layers were completely transparent at wavelengths longer than 900 nm, and the absorption at these wavelengths occurred at the Schottky metal only.

The samples were fabricated by a microwave-compatible process. Initially the resonance of the cavity was tuned to 1.3 μm with a recess etch. Then, ohmic contacts to the n^+ layers were formed by a self-aligned Au–Ge–Ni lift-off process. The samples were rapid thermal annealed at 450 °C for 45 s. Using an isolation mask, we etched away all of the epilayers except the active areas. We then evaporated Ti/Au interconnect metal to form coplanar waveguide (CPW) transmission lines on top of the semi-insulating substrate. The next step was the evaporation of a 10-nm-thick Au Schottky layer on top of the n^- layer followed by sputtering of a 100-nm-thick indium tin oxide (ITO) layer. Au and ITO layers formed the top mirror of the cavity. Then a 370-nm-thick Si_3N_4 layer was deposited and patterned. Besides passivation and protection of the surface, Si_3N_4 was also used as the dielectric layer of the metal–insulator–metal bias capacitor. Finally, a 0.8-μm-thick Au layer was deposited as an airbridge to connect the center of CPW to the Schottky layer. The airbridge process was essential to obtain high speed devices with very low parasitic capacitances. The cross section of a fabricated photodiode is shown in Fig. 2.

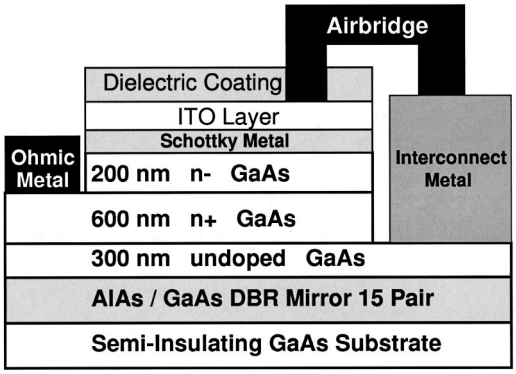

FIG. 2. Cross section of a fabricated RCE photodiode.

Photoresponse measurements were carried out in the 1100–1500 nm range by using a single-pass monochromator and a tungsten-halogen projection lamp as the light source. The output of the monochromator was coupled to a 62.5 μm diameter multimode fiber. The monochromatic light was delivered to the devices by a lightwave fiber probe, and electrical characterization was carried out on a probe station. The spectral response was measured using a calibrated optical powermeter. For spectral measurements, large-area photodiodes (150 μm$\times$150 μm) were chosen to ensure all of the optical power was incident on the active area. Figure 3(a) shows the spectral room temperature quantum efficiency measurement and theoretical calculations at zero bias. When compared with a single-pass structure, the enhancement factor of the device is $\sim$9 at the resonant wavelength. The peaks in the spectrum are due to the resonance of the cavity and the reflection dips. The deviation from the theoretical calculations can be due to the roughness of the Au Schottky layer.

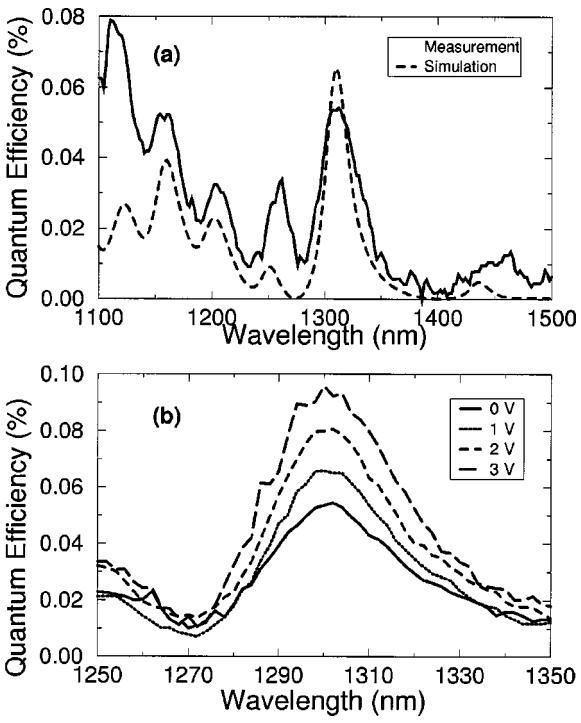

FIG. 3. (a) Measurement and simulation of spectral quantum efficiency at room temperature. (b) Room temperature measurement of spectral quantum efficiency at various reverse biases. The peak quantum efficiency at the resonance wavelength increases with bias.

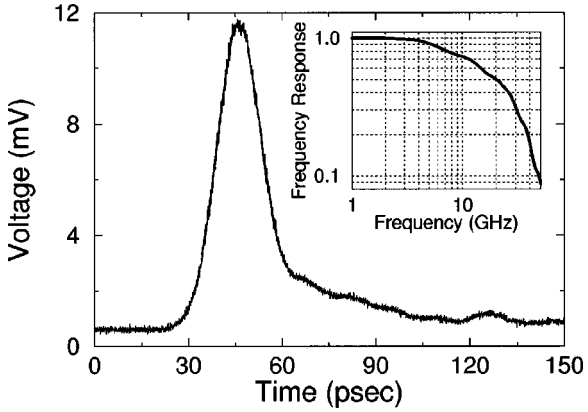

FIG. 4. Temporal response of the 100 μm^2 area RCE Schottky photodiode. The inset shows the calculated frequency response of high-speed measurement data.

We have also investigated the effect of reverse bias on quantum efficiency. Figure 3(b) shows the measured quantum efficiency at various reverse bias voltages. The increase in quantum efficiency with the bias voltage can be explained by the decrease of the Schottky barrier, which in turn increases the cutoff wavelength. The peak quantum efficiency (0.1%) that we have obtained from our devices was comparable to the quantum efficiency performance obtained from silicide-based internal photoemission Schottky detectors, where a peak quantum efficiency of 0.2% had been reported.[16]

High-speed measurements were made with an optical parametric oscillator (OPO)[17] used as the ultrafast light source. Our OPO was based on a periodically poled $KTiOPO_4$ crystal with a 24 μm poling period, and was pumped by a mode-locked Ti:sapphire laser operating at a wavelength of 762 nm with 215 fs in duration and had a repetition rate of 76 MHz. The OPO produced pulses at 1310 nm with a full width at half maximum pulse width less than 1 ps. The OPO output was coupled to a single mode fiber, and the signal was delivered to the devices by a lightwave fiber probe. Figure 4 shows the temporal response of a small area ($7\ \mu m \times 13\ \mu m$) photodiode measured by a 50 GHz sampling scope at zero bias. As shown in the inset of the Fig. 4, the Fourier transform of the measurement data has a 3 dB bandwidth of 20 GHz. Considering the measurement setup limitations, laser timing jitter, and the dimensions of the device under test, we estimate the actual frequency response of the device to be around 50 GHz. These results correspond to the first high-speed internal photoemission photodetectors published in scientific literature.

In conclusion, we have demonstrated a 1.3 μm high-speed resonant cavity enhanced GaAs based Schottky barrier internal photoemission photodetector. The device exhibited a temporal response of 16 ps which was limited by the experimental setup.

This work is supported by Turkish Department of Defense Grant No. KOBRA-001, NATO Grant No. SfP971970, and National Science Foundation Grant No. INT-9906220.

[1] M. Razeghi, in *Long Wavelength Infrared Detectors*, edited by M. Razeghi (Gordon and Breach, The Netherlands, 1996), pp. ix–xiii.
[2] R. T. Carline, V. Nayar, D. J. Robbins, and M. B. Stanaway, IEEE Photonics Technol. Lett. **10**, 1775 (1998).
[3] J. S. Park, T. L. Lin, E. W. Jones, H. M. D. Castillo, and S. D. Gunapala, Appl. Phys. Lett. **64**, 2370 (1994).
[4] W. Z. Shen, A. G. U. Perera, H. C. Liu, M. Buchanan, and W. J. Shaff, Appl. Phys. Lett. **71**, 2677 (1997).
[5] A. G. U. Perera, H. X. Yuan, S. K. Gamage, W. Z. Shen, H. M. Francombe, H. C. Liu, M. Buchanan, and W. J. Schaff, J. Appl. Phys. **81**, 3316 (1997).
[6] H. X. Yuan and A. G. U. Perera, Appl. Phys. Lett. **66**, 2262 (1995).
[7] A. G. U. Perera, W. Z. Shen, H. C. Liu, M. Buchanan, M. O. Tanner, and K. L. Wang, Appl. Phys. Lett. **72**, 2307 (1998).
[8] B. Y. Tsaur, M. M. Weeks, R. Tubiano, P. W. Pellegrini, and T. R. Yew, IEEE Electron Device Lett. **9**, 650 (1988).
[9] M. S. Unlu and S. Strite, J. Appl. Phys. **78**, 607 (1995).
[10] H. Nie, K. A. Anselm, C. Hu, S. S. Murtaza, B. G. Streetman, and J. C. Campbell, Appl. Phys. Lett. **70**, 161 (1997).
[11] C. Lennox, H. Nie, P. Yuan, G. Kinsley, A. L. Holmes, Jr., B. G. Streetman, and J. C. Campbell, IEEE Photonics Technol. Lett. **11**, 1162 (1999).
[12] M. S. Unlu, M. Gokkavas, B. M. Onat, E. Ata, E. Ozbay, R. P. Mirin, K. J. Knopp, K. A. Bartness, and D. H. Christensen, Appl. Phys. Lett. **72**, 2727 (1998).
[13] E. Ozbay, I. Kimukin, N. Biyikli, O. Aytur, M. Gokkavas, G. Ulu, M. S. Unlu, R. P. Mirin, K. A. Bertness, and D. H. Christensen, Appl. Phys. Lett. **74**, 1072 (1999).
[14] R. H. Fowler, Phys. Rev. **38**, 45 (1931).
[15] G. Gigli, M. Lomascolo, M. D. Vittorio, R. Cingolani, A. Cola, F. Quaranta, L. Sorba, B. Mueller, and A. Franciosi, Appl. Phys. Lett. **73**, 259 (1998).
[16] T. L. Lin and J. Maserjian, Appl. Phys. Lett. **57**, 1422 (1990).
[17] T. Kartaloglu, K. G. Koprulu, O. Aytur, M. Sundheimer, and W. P. Risk, Opt. Lett. **23**, 61 (1998).